Estimation of Troposphere Decorrelation Using the Combined Zenith-dependent Parameter

Yong Won Ahn, Don Kim and Peter Dare
Geodetic Research Laboratory, Department of Geodesy and Geomatics Engineering,
University of New Brunswick, Fredericton, New Brunswick, Canada

James Park
Space Geodesy Division, Korea Astronomy and Space Science Institute, Daejeon, South Korea

BIOGRAPHIES

Yong Won Ahn holds an M.Sc from the Department of Geomatics Engineering at the University of Calgary awarded in 2005. He is currently a Ph.D candidate in the Department of Geodesy and Geomatics Engineering at the University of New Brunswick (UNB). His current research focuses on the tropospheric anomaly effect on RTK system.

Don Kim is a Senior Research Associate and a faculty member in the Department of Geodesy and Geomatics Engineering at the University of New Brunswick (UNB). He has a bachelor's degree in urban engineering, and an M.Sc.E. and Ph.D. in geomatics from Seoul National University. He has been involved in GPS research since 1991 and active in the development of an ultrahigh-performance RTK system for the past few years. He received the Dr. Samuel M. Burka Award for 2003 from The Institute of Navigation (ION). He also shared two IEEE/ION PLANS Best Track Paper Awards for 2006 and 2008.

Peter Dare is the Chair of the Department of Geodesy and Geomatics Engineering at UNB. He obtained a B.Sc. (Hons) in Land Surveying Sciences from North East London Polytechnic in 1980, an M.A.Sc. in Civil Engineering from the University of Toronto in 1983 and a Ph.D. in geodesy from the University of East London in 1996. He joined UNB in 2000 and became the Chair of the Department in 2002. He was elected a Fellow of the Royal Institution of Chartered Surveyors (RICS) in 2000.

James Park is a principal research scientist (division director) at the GNSS division of Korea Astronomy and Space Science Institute. He holds a B.Sc, an M.Sc, and a Ph.D in Astronomy and Space Science from Yonsei University in South Korea. He has been involved with GNSS research since 1993 and his current research interests are the development of GNSS networks for high precision GNSS positioning and its real-time application systems.

ABSTRACT

For dual-frequency GPS observables, one of the largest error sources affecting high-precision positioning solutions arises from the unmodelled troposphere. Even for the short baseline, the resultant solution can be degraded once there is strong anomaly effect due to the troposphere. The problem can be more difficult as the troposphere parameters are highly correlated with the height component.

In order to decorrelate those parameters, we introduce a new approach in this paper. Instead of two separate parameters, we combine them into one common parameter as they are both zenith-dependent parameters. We have examined the feasibility of our proposed method for estimating the positioning and residual troposphere parameters. Data collected in Southern Texas, USA, on August 21, 2005 over a baseline length of around 7.8 km was reprocessed.

The positioning solution from the new combined proposed parameter has been tested, evaluated, and compared with that from the conventional estimation method. By using the methodology, significant positioning improvement was achieved in the horizontal component as well as the vertical component. Also, the estimated troposphere parameters using the combined parameter are compared with that from the uncombined parameter.

INTRODUCTION

Atmospheric effects, including the ionosphere and the troposphere, are one of the most significant error sources in global navigation satellite system (GNSS) real-time kinematic (RTK) positioning and navigation. In the case of the troposphere, almost 90% of the total delay occurs in the hydrostatic component, which varies slowly with time. This hydrostatic delay can be easily modeled with the assumption of hydrostatic equilibrium to an accuracy at the millimetre level [Mendes and Langley, 1995]. Unlike the hydrostatic part, the non-hydrostatic (or wet) part has strong spatial and temporal variations. The effects of wet delay to

the range can reach 10-40 cm. Large residual errors in modeling can cause significant errors in high-precision GNSS positioning applications. To reduce or minimize these errors arising from poor modeling of the wet troposphere, one possibility is to model the tropospheric refraction using a purely independent data set without GNSS observations. The other approach is to estimate the tropospheric parameters directly using the available GNSS data. Due to their spatial and temporal correlation characteristics, these errors can be substantially minimized under short-baseline situations by differential techniques.

When a strong tropospheric anomaly exists within a network, however, the differential errors cannot be reduced to a negligible level even under short-baseline situations. These errors can adversely affect the rover positioning solution and also make the entire network solutions unreliable.

Some previous studies on the troposphere (e.g., Skone and Shrestha, 2003; Nicholson *et al*., 2005) have been focused mainly on tropospheric delay estimation for the atmospheric sciences. These include the atmosphere tomography for modeling the atmosphere. Meanwhile, the GNSS positioning community has been concerned about how well the tropospheric delay can be modeled for high-precision positioning. For relative positioning, double differencing (DD) between satellites and receivers can generally provide more reliable solutions than precise point positioning (PPP). Some studies have focused on independent observables (e.g., water vapor from a water vapor radiometer) to retrieve the absolute atmospheric parameters for other stations. In addition, a recent achievement includes a ray-tracer based on a numerical weather prediction model (e.g., Rapid Update Cycle 13 km (RUC13) by National Oceanic and Atmospheric Administration (NOAA) in USA, and Global Environmental Multiscale (GEM) NWP model from the Canadian Meteorological Centre of Environmment Canada) [Cove *et al*., 2004; Ahn *et al*., 2005; Cove, 2005; Nievinski *et al*., 2005]. For sparse areas, it gives an independent measurement of the tropospheric delays. From a practical point of view, however, the ray-tracer has its limitations such as its latency and real-time data reception issue. In addition, the grid spacing currently adopted is too large to consider a locally anomalous atmospheric condition.

Previous Research on Atmospheric Anomalies

One of the localized anomalies could be observed at Stennis Continuously Operating Reference Stations (CORS) in Texas, USA. The baseline length is about 2.1 km which is short enough to eliminate the correlated errors in the atmosphere. During the time when there was a localized troposphere anomaly at 20 hours UTC (see Figure 1), the residuals reached over a half cycle, thus causing a failure to resolve ambiguities successfully.

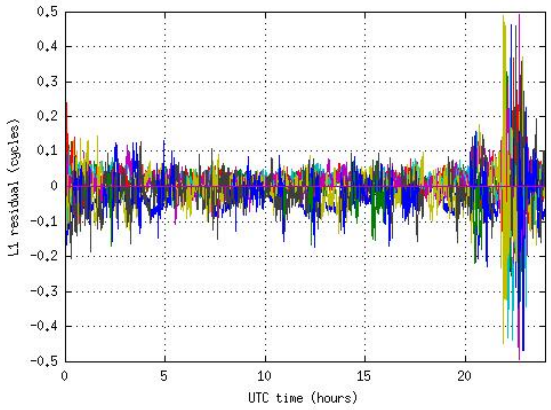

Figure 1. L1 DD residuals on Stennis CORS Stations in Texas on 21st August in 2005. The baseline length is 2.1 km [Lawrence *et at.*, 2006].

Similar weather could be observed near San Marcos CORS stations, CSM1 and TXSM in Texas on 11th October 2005 over a 2.7 km baseline length. During passage of the localized storm, the GPS RTK performance seemed to be much degraded mainly due to the wrongly fixed ambiguities, resulting in corrupting the positioning performance as well. Figure 2 shows the L1, L2, and wide-lane DD residual for the satellite pair PRN20 and PRN25.

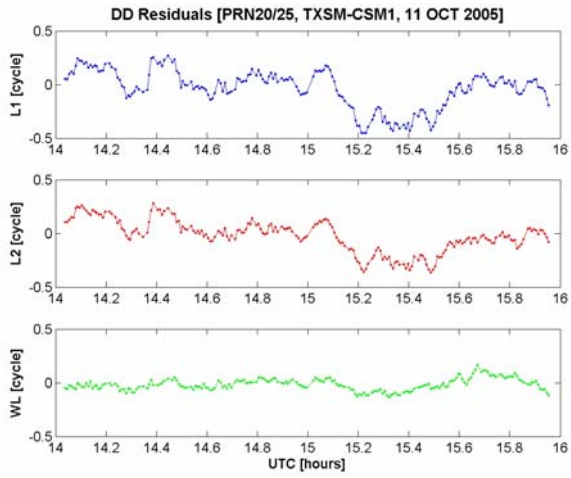

Figure 2. L1, L2, and wide-lane residuals on San Marcos CORS stations, TXSM and CSM1, in Texas, observed on 11th October 2005. The baseline length is 2.7 km.

The residual zenith delay of the troposphere and the height component of the positioning solutions are highly dependent on the zenith angle. Due to their correlation, most of the position estimation errors induced by the troposphere are amplified mainly in the vertical component. Depending on weather conditions, a stochastic modeling approach or parametric estimation has been implemented to decorrelate or mitigate the tropospheric error for medium length baselines. However, the case will be substantially

different when a local tropospheric anomaly exists in a network.

Our previous research on a similar topic investigated the use of additional tropospheric parameters such as residual zenith tropospheric delay and horizontal gradient parameters [Ahn *et al.*, 2007]. Although our previous approach was successful in reducing the tropospheric residuals and thus resulted in an improvement in the solution domain, this approach has two main limitations from practical aspects. First, the additional parameters may degrade the entire positioning solution in the estimation process due to redundancy and inter-correlation of parameters. Second, an arbitrary choice of the parametric spacing for the residual troposphere or the gradient estimation is not practical.

MOTIVATION

An inhomogeneous atmospheric phenomenon has been frequently observed in many different networks around the world. These include severe sand, dust storms, volcanic eruptions, ionospheric scintillation effects, and localized or regional tropospheric anomaly effects [Comparetto, 1993]. Occasionally, these phenomena are observed when a strong tropospheric anomaly exists within a network. As stated, even for a short baseline, imbalanced atmospheric errors are shown to have a severe impact on rover positioning solutions, resulting in a worsening of the quality of the positioning solutions [Ahn *et al.*, 2006; Lawrence *et al.*, 2006; Zhang and Bartone, 2006; Huang and van Graas, 2006; Kim and Langley, 2007].

A very strong localized tropospheric anomaly was observed in Southern Texas on August 21, 2005. Over a baseline length of around 7.8 km, the atmospheric effects should be highly correlated and thus easily eliminated in double-differencing (DD). However, the DD residuals of the carrier-phase measurements reached over 50 ppm and most of the carrier-phase ambiguity resolutions on those specific periods failed in Bernese (software version 5.0). As expected, the errors created by mis-modeling the troposphere are propagated into the vertical component. During this process, we also introduced the residual zenith tropospheric delay and the horizontal gradient parameters to estimate the rover position. We find they are not very helpful in reducing the errors.

The possibility of other error sources combining with the water droplets (e.g. sand and hydrometeors) has been also investigated. In order to evaluate the sand and dust effect, various sparse network data from a CORS network in Texas on 24th February 2007 had been reprocessed using Bernese GPS software v5.0. A large dense blowing dust storm was observed across the middle of Texas moving into southwestern Oklahoma on that day. This phenomenon was observed by a Moderate Resolution Imaging Spectroradiometer (MODIS) instrument and an image was provided by National Aeronautics and Space Administration (NASA). However, we concluded that the effect of sand and dust, combined with the water droplets, could be hardly observed for those specific GPS frequencies.

Under extremely inhomogeneous conditions in the lower troposphere, a physical interpretation may be difficult, if not impossible to evaluate, resulting in certain misassumption about the parametric model. Therefore, not only was a residual analysis of the tropospheric delay carried out, but also a new approach to combine zenith dependent parameters into one common parameter is studied – this is to avoid incorrect tropospheric modeling. As is shown in Figure 3, both the height component and the residual tropospheric component are highly dependent on the zenith angle.

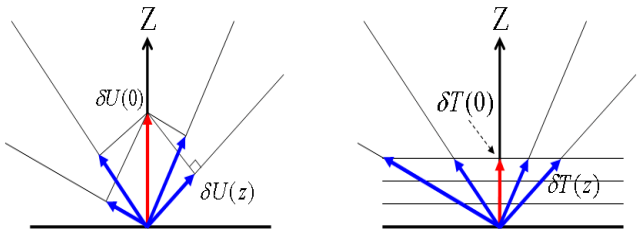

(Z. Dependency of height) (Z. Dependency of trop.)

$$\delta U(z) = \cos(z) \cdot \delta U(0) \qquad \delta T(z) = \frac{1}{\cos(z)} \delta T(0)$$

Figure 3. Zenith dependency for both vertical component and the tropospheric delay parameter

The combined approach can eliminate inter-correlation among zenith angle-dependent parameters and thus, improve horizontal positioning solutions. This can result in the successful decorrelation of both the vertical component and the troposphere delay parameter.

METHODOLOGY

The DD carrier-phase observations are used in our approach. Assuming that the carrier phase ambiguities are correctly resolved and accurate meteorological data are available at a reference station and a rover, we will have a reduced GPS carrier-phase observation model for short-baseline applications as:

$$\begin{aligned} &\lambda_{L1}\varphi_{AB}^{jk}(t) - \lambda_{L1}N_{AB}^{jk} - \rho_{AB_0}^{jk} - T_{AB}^{jk} \\ &= h_x^{jk}\Delta X_B + h_y^{jk}\Delta Y_B + h_z^{jk}\Delta Z_B + m_B^{jk}(t)\tau_{AB}(t) + e \end{aligned} \quad (1)$$

$$h_x^{jk} = -\frac{X^k(t) - X_{B_0}}{\rho_{B_0}^k(t)} + \frac{X^j(t) - X_{B_0}}{\rho_{B_0}^j(t)}$$

$$h_y^{jk} = -\frac{Y^k(t) - Y_{B_0}}{\rho_{B_0}^k(t)} + \frac{Y^j(t) - Y_{B_0}}{\rho_{B_0}^j(t)}$$

$$h_z^{jk} = -\frac{Z^k(t) - Z_{B_0}}{\rho_{B_0}^k(t)} + \frac{Z^j(t) - Z_{B_0}}{\rho_{B_0}^j(t)},$$

where

λ_{L1} : L1 wavelength (metres)

φ_{AB}^{jk} : DD phase observables (cycles): superscripts j and k stands for the satellites, and subscripts A and B for the receivers

N_{AB}^{jk} : DD integer carrier phase ambiguities (cycles)

ρ_{AB}^{jk} : DD geometric range (metres)

T_{AB}^{jk} : DD hydrostatic (or dry) delay (meters)

X^k , Y^k , Z^k : satellite positions in Earth-centered Earth-fixed (ECEF) coordinate system (metres)

X_{B0} , Y_{B0} , Z_{B0} : approximate receiver positions in ECEF coordinate system (metres)

ΔX_B , ΔY_B , ΔZ_B : receiver position increments (metres)

m_B^{jk} : single-differenced (between satellites) non-hydrostatic (or wet) mapping coefficient at the receiver B (unitless)

τ_{AB} : relative wet zenith delay (metres)

e : residual errors (e.g., receiver system noise, multipath, etc.)

Under short baselines, the residual effects of the ionosphere and troposphere are typically insignificant. As we are dealing with a strong anomaly effect in the lower troposphere, the residual tropspheric term (without the assumption of atmospheric azimuthal asymmetry and use of gradient estimation) is included in order to have a more realistic equation. The above equation can be expressed in vector-state form as follows:

$$\mathbf{L} = \mathbf{H}\mathbf{x} + \mathbf{m}\tau + \mathbf{e}, \qquad \mathbf{e} \sim N(\mathbf{0}, \mathbf{Q_L}) \tag{2}$$

where

$$\mathbf{L} = \lambda_{L1}\boldsymbol{\varphi}_{AB}^{jk}(t) - \lambda_{L1}\mathbf{N}_{AB}^{jk} - \boldsymbol{\rho}_{AB_0}^{jk} - \mathbf{T}_{AB}^{jk}$$

$$\mathbf{H} = \begin{bmatrix} \mathbf{h}_x & \mathbf{h}_y & \mathbf{h}_z \end{bmatrix} \tag{3}$$

$$\mathbf{x} = \begin{bmatrix} \Delta X_B & \Delta Y_B & \Delta Z_B \end{bmatrix}^T$$

Note that **e** is a normally distributed random vector with expected value of **0** and variance-covariance $\mathbf{Q_L}$.

In order to analyze the common zenith dependent parameters (that is, the vertical component of the receiver's position and the wet zenith delay), the local geodetic coordinate system is introduced. The axes *n* and *e* span the local geodetic horizon which is perpendicular to the ellipsoidal normal through the surface of point P as illustrated in Figure 4. In Figure 4, *n* and *e* point north and east, and *u* coincides with the ellipsoidal normal with the positive end upward of the ellipsoid [Leick, 1995].

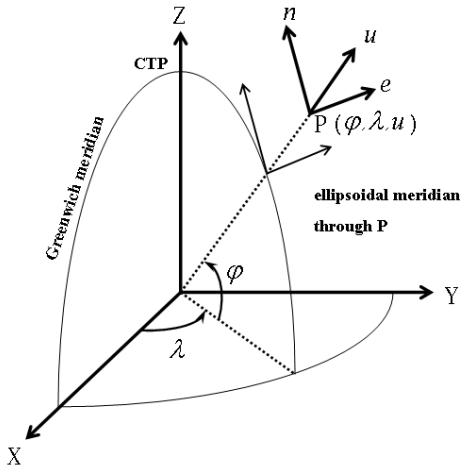

Figure 4. Local geodetic coordinate system

The relationship between the local geodetic coordinate system and the geocentric system is as follows:

$$\mathbf{x} = \mathbf{R}^{-1}\mathbf{n}$$

$$\mathbf{R} = \begin{bmatrix} -\sin\varphi\cos\lambda & -\sin\varphi\sin\lambda & \cos\varphi \\ -\sin\lambda & \cos\lambda & 0 \\ \cos\varphi\cos\lambda & \cos\varphi\sin\lambda & \sin\varphi \end{bmatrix} \tag{4}$$

$$\mathbf{n} = \begin{bmatrix} \Delta n & \Delta e & \Delta u \end{bmatrix}^T$$

where **R** is the rotation matrix and **n** is a vector of the position component increments in local geodetic system. Given the latitude and longitude of the receiver, the geocentric coordinate system can be easily transformed to the local geodetic system based on Equation (4). Equation (2) can be now rewritten as a sub-matrix forms as follows:

$$\mathbf{L} = \mathbf{G}\mathbf{n} + \mathbf{m}\tau + \mathbf{e}$$

$$= \begin{bmatrix} \mathbf{g}_n & \mathbf{g}_e \end{bmatrix}\begin{bmatrix} \Delta n \\ \Delta e \end{bmatrix} + \begin{bmatrix} \mathbf{g}_u & \mathbf{m} \end{bmatrix}\begin{bmatrix} \Delta u \\ \tau \end{bmatrix} + \mathbf{e} \tag{5}$$

$$\mathbf{G} = \mathbf{H}\mathbf{R}^{-1}$$

Equation (5) gives a straightforward interpretation of the vertical increment Δu and the wet zenith delay τ . Figure 5 shows the relationship between the vertical component of the design matrix $\mathbf{g}_u$ and the Niell's wet mapping function

coefficient **m** [Niell, 1996] for each satellite. As illustrated in Figure 5, they are correlated with each other, especially at the high elevation angles. For comparison purpose, we used the '*negative*' Niell wet mapping coefficients at the right-side y-axis in Figure 5. The functional relationship between the two coefficients is illustrated in Figure 6. As implied in Figure 6, the two parameters (the vertical increment and the wet zenith delay) will have strong correlation at high elevation angles. On the other hand, their correlation becomes weaker at lower elevation angles.

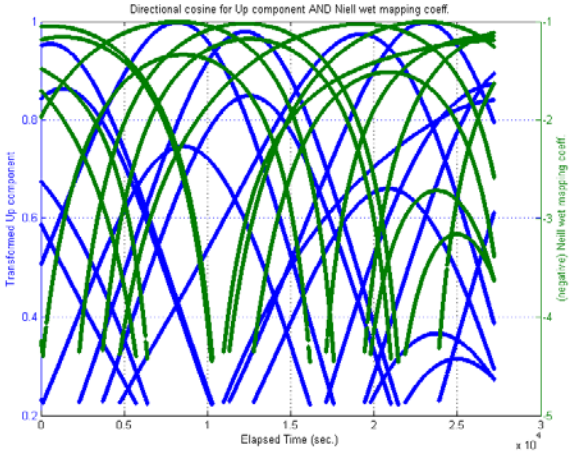

Figure 5. Relationship between the vertical component $\mathbf{g}_u$ and the Niell's wet mapping coefficient $\mathbf{m}$.

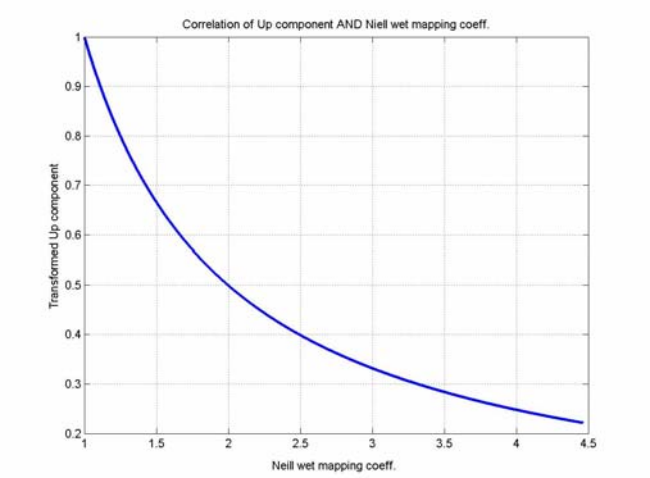

Figure 6. Functional relationship between the vertical component $\mathbf{g}_u$ and the Niell's wet mapping coefficient $\mathbf{m}$.

The challenge we try to overcome in this paper is to break-up the correlation between the two parameters (the vertical increment and the wet zenith delay). Even if they have a functional relationship with each other, the two parameters cannot be easily combined into one single parameter and probably even impossible to have a linearized form. Therefore, we follow a numerical approach to solve the the correlation problem in this study. By introducing the new parameters, α and ζ, the two parameters can be combined as follows:

$$\mathbf{g}_u \Delta u + \mathbf{m}\tau = \left[\alpha \mathbf{g}_u + (1-\alpha)\mathbf{m}\right]\zeta \qquad (6)$$

where

$$\alpha = \frac{\Delta u}{(\Delta u + \tau)}, \qquad \zeta = (\Delta u + \tau).$$

The α represents the ratio between the vertical component increment and ζ. Typically, α has the value $0<\alpha \le 1$. By changing the α from 0 to 1 with a step size of 0.01, we can find the best positioning solution among 100 different solutions. An example is illustrated in Figure 7. By changing the value of α, we can adjust the weight of the two parameters. In Figure 7, there is a point which minimizes the weighted sum of the squared residuals. Choosing a different α will give a different solution (e.g. much worse or much better) as they weigh differently the vertical component of the design matrix $\mathbf{g}_u$ and the Niell's wet mapping function coefficient $\mathbf{m}$.

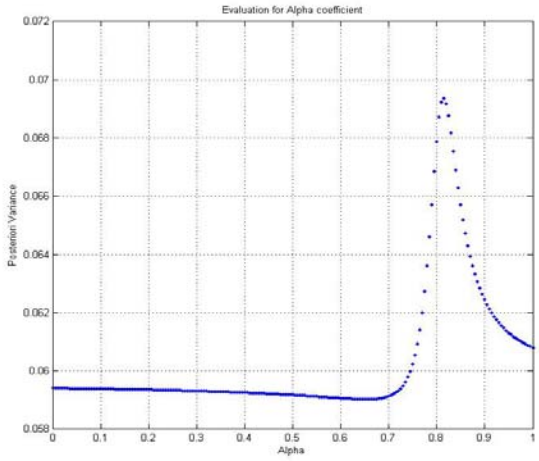

Figure 7. Weighted sum of the squared residual corresponding to α from 0 to 1 with a step size of 0.01. This is a single epoch example.

DATA DESCRIPTION & PROCESSING STRATEGY

To evaluate the potential improvement of positioning performance by combining the common zenith dependeant parameter of the vertical component and the residual tropospheric delay parameter, we analyzed a severe weather event. These data were recorded in Southern Texas on August 21, 2005. The baseline length was of around 7.8 km. All of the data sets were recorded using the NovAtel™ OEM4 receiver with a data rate of 1 Hz. The observation time is almost 8 hours. Figure 8 illustrates the approximate location [Google, 2008], and there are no buildings or trees

near the two reference sites which can usually cause multipath, cycle slips, etc. The image in Figure 9 is an infrared satellite and radar image on the same day; a strong atmospheric effect can be observed.

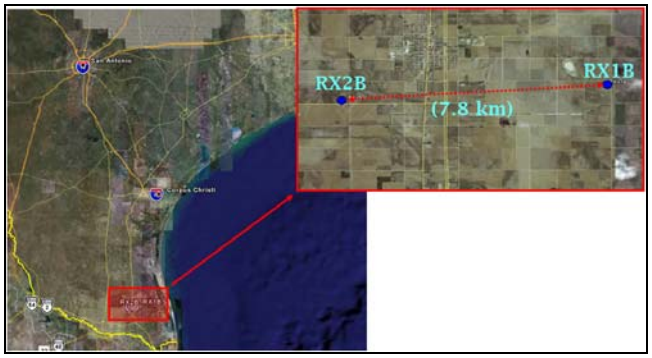

Figure 8. Geographic location of the two sites, RX1B and RX2B, studied [Google, 2008].

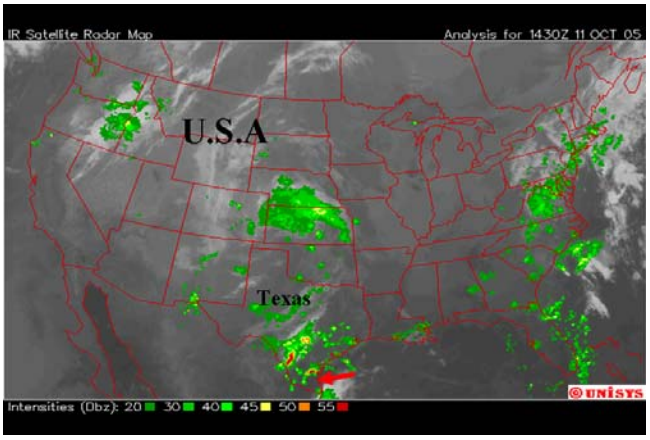

Figure 9. Satellite infrared image and radar map [UNISYS, 2005].

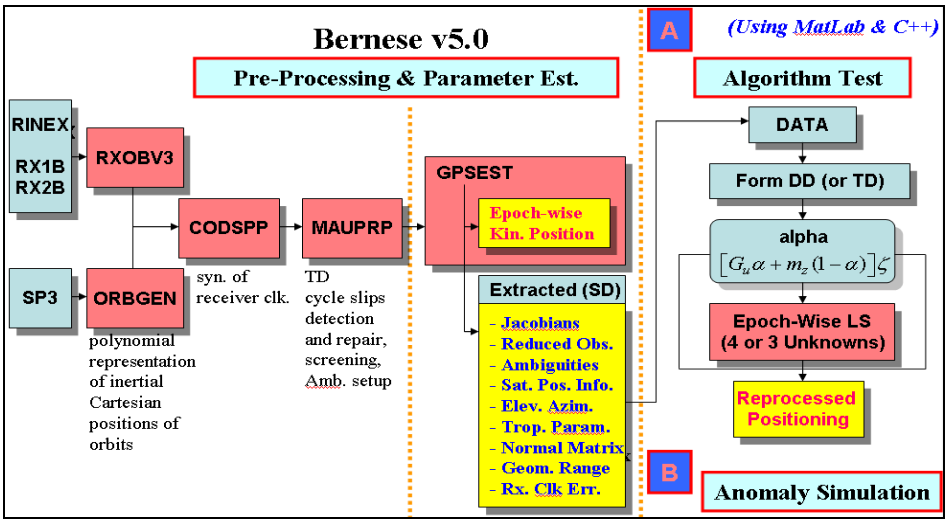

Figure 10. Processing strategy.

The processing is based on double differences. For processing the GPS data, Bernese software version 5.0 was used to extract the desired parameters for further analysis using our methodology described earlier. Figure 10 represents the processing scheme. Once the baseline was formed, cycle slips were correctly detected and repaired. Then, L1 (and L2) ambiguities were resolved using an ambiguity search process. After all possible ambiguities were resolved, these ambiguities were introduced to obtain the final positioning solutions. At the same time, the residual troposphere parameters at 15 minutes intervals were estimated. In order to analyze our methodology, several parameters at single difference level were extracted; Jacobians, reduced observables, ambiguities, satellite positions, elevation and azimuth of the satellites, tropospheric parameters, normal matrices, geometric ranges, receiver clock, etc. Selected parameters are used as input parameters for the algorithm test. The primary reason for choosing this methodology is to minimize uncertainties in the data analysis and maximize the performance analysis in using geodetic software. After reforming the double differences, 100 different α were tested for every epoch. Once the value of α is selected using a selection criteria, the determined α is used again to get the final positioning solution and the residual troposphere delay parameter. For the comparison, the solution for the 4 unknown parameters (northing, easting, up, and residual troposphere) are generated, as well as the three unknown parameters (northing, easting, and ζ). As is in Equation (6), if α and ζ are determined, new tropospheric estimates can be retrieved based on the relation: $\zeta = \left(\Delta u + \Delta \tau_z\right)$. During Bernese data processing, IGS final SP3 orbit products were used to mitigate the possible residual orbit errors.

The other test is to simulate the similar atmospheric anomaly effect using a hardware simulator. The estimated

15 minute residual tropospheric delay values and the corresponding L1 residuals from the Bernese software were introduced together into the Spirents™ Communications STR4760 L1, L2, L2C dual hardware simulator as a modeled troposphere.

RESULTS

Figure 11 represents the L1 double differenced residuals processed by Bernese. During the processing RX1B is used as a reference, and RX2B is selected as a rover. The solution is based on the post-processed kinematic scenarios. We introduced the dry Niell mapping function with the dry Saastamoinen model [Saastamoinen, 1972], and estimated 15 minute residual tropospheric delay parameters. In order to try to obtain a better solution, we tested a few other processing strategies. These strategies include the ionosphere-free linear combination to eliminate the first order ionosphere effect even if the noise level is almost three times higher than that of L1. L2 and wide-lane combination was also processed. However, we could not get the residuals less than 50 ppm with the different methodologies. Figure 11 represents the investigated satellites. As is illustrated, the problematic satellites are PRN 24 and PRN 19 which are lower elevation angles, and we found that the corresponding elevation angles are between 15 and 30 degrees.

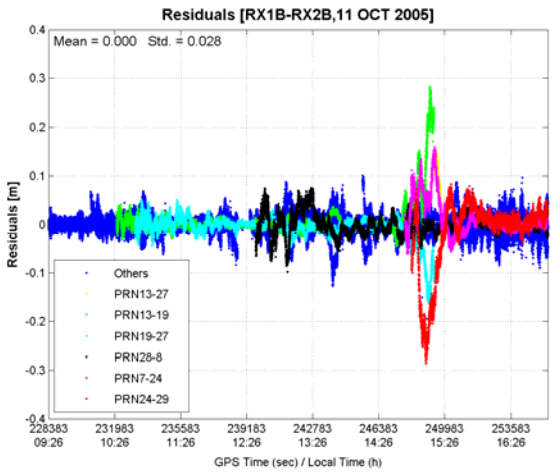

Figure 11. L1 double difference residuals by Bernese kinematic scenario.

To evaluate the correlation effect between the unknown parameters, the condition number is also examined as is illustrated in Figure 12. The condition number is the ratio of maximal and minimal eigenvalue of a normal matrix. This also represents the degree of the correlation between the parameters. As is shown, the condition number increases from 13:00 (local time) which means that the correlation between the unknown parameters is getting higher, resulting in a degraded solution. Typically, introducing a lower satellite can assist in decorrelating the parameters. Figure 13 represents the corresponding kinematic positioning solutions. We can see the solution getting worse after 13:00 (local time), especially in the vertical component.

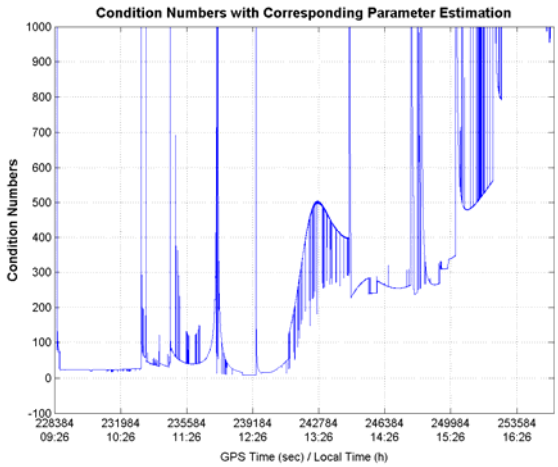

Figure 12. Condition number from Bernese software

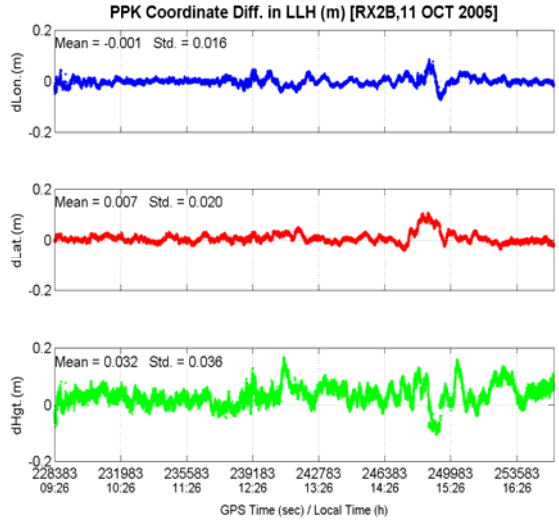

Figure 13. Kinematic positioning solutions by Bernese software.

Figure 14 is a test result of a kinematic positioning solution for a typical estimation process where there are four unknown parameters; northing, easting, up, residual tropospheric delay. We expected to have the same positioning result as that from Bernese software in Figure 13. However, there are slightly different coordinate results; they are probably due to the wrongly indexed fixed cycle slips. However, the reprocessed result shows the high fluctuation of the solution when there is the troposphere anomaly.

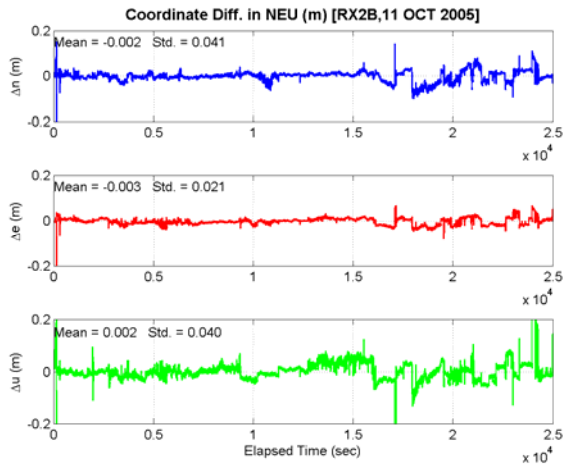

Figure 14. The coordinate differences of northing, easting, and up component. This result is from the conventional way for estimating the unknown parameters, *"without"* any combination between the parameters.

Figure 15 is a test result from our combined methodology when all of the necessary parameters used are reprocessed. The three parameters that were estimated are northing, easting, and ζ. Once ζ was determined based on the selected α, the vertical component was retrieved. The choice of α coefficient is somewhat arbitrary, and there is no strict numerical way to determine the α coefficient. In this research, we chose α when the norm of the coordinate solutions is at minimum value. As we focused on the static scenario, it is relatively easy to choose the α compared to that in the kinematic scenario. As is shown in Figure 15, when α is 'properly' chosen, the corresponding coordinate solution can dramatically change and converge to the known positioning solution.

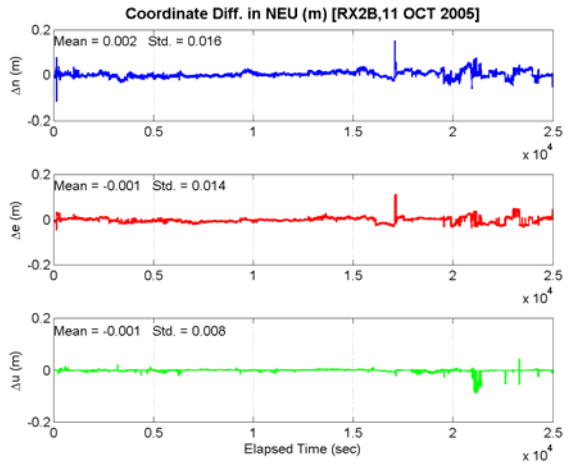

Figure 15. The coordinate differences of northing, easting, and up component. This result is from the combined case to estimate three unknowns, *"with"* the combination between the parameters.

Figure 16 represents the two estimated tropospheric parameters either from the typical estimation process (red line) or from the combined methodology (blue line). Once ζ was determined based on the selected α, the tropospheric delay parameters can be also retrieved. These values are colored blue in the figure. As a comparison, the tropospheric delay parameters are also estimated using a typical method of estimation. As is shown, there are big differences between the estimated tropospheric delay parameters. By using a different tropospheric weighting scheme based upon α, the estimator seems to enable us to efficiently distinguish the tropospheric delay parameters from the unmodelled height component as seen from Figure 15 and Figure 16.

We also simulated similar troposphere anomaly effects using our hardware simulator. The estimated 15 minute residual tropospheric delay values and the corresponding L1 residuals from the Bernese software are also incorporated into Spirents™ STR4760 dual hardware simulator. The primary goal is to create a similar phenomenon by simulation based on the known values of the troposphere. The SimGNSS™ simulator control software for the simulator enables it to be setup with many different test environments. Instead of implementing many different errors, such as orbit perturbations, clock errors, ionospheric errors, multipath, etc, the errors implemented in this study are both 1 Hz tropospheric delays with L1 double difference residuals, with the antenna gain pattern.

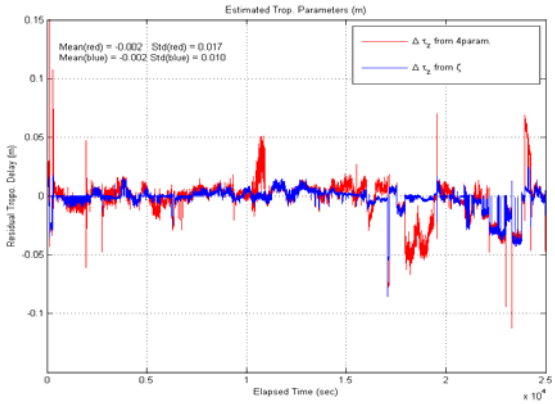

Figure 16. The estimated tropospheric delay parameters from combined ζ unknowns (colored in blue). The red line represents when the tropospheric parameters are directly estimated without any modification in a typical estimation process.

For the antenna, we simulated a gain pattern for NovAtel™ GPS 600G. Figure 17 illustrates the hardware simulator setup. Figure 18 represent the simulated antenna gain pattern for the GPS 600G model.

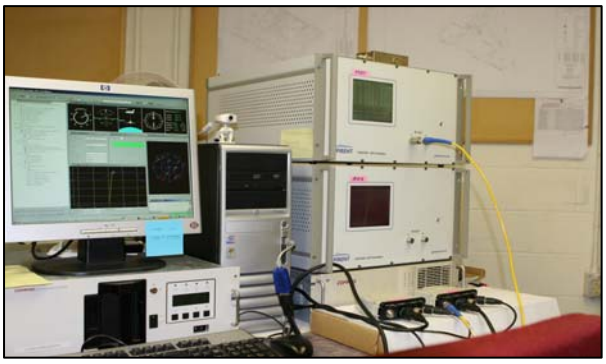

Figure 17. Spirent™'s STR4760 dual hardware simulator at the GNSS Simulation and System Integration Lab. in the Department of Geodesy and Geomatics at the University of New Brunswick.

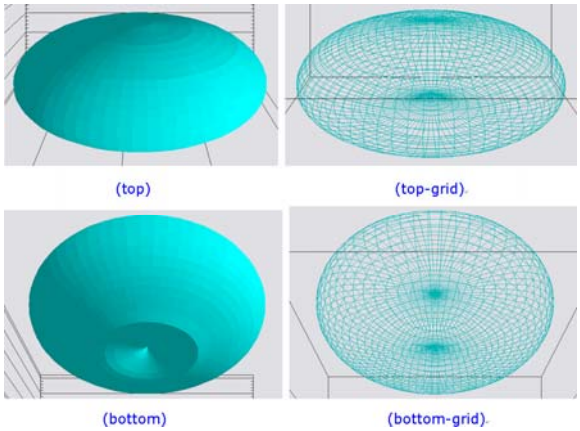

Figure 18. The simulated NovAtel™ GPS 600-G antenna gain pattern.

Based on the parameters stated above, the simulation was performed. Figure 19 and Figure 20 illustrate the estimated vertial differences and the residuals from the kinematic positioning solution for the simulated RX2B once the simulated RX1B has been fixed as a reference. For the purpose of the anomaly scenario, we introduced a severe tropospheric effect to the simulator between epochs 6000 and 8000 (in seconds). As is shown in the plot, the solution is getting worse during these times.

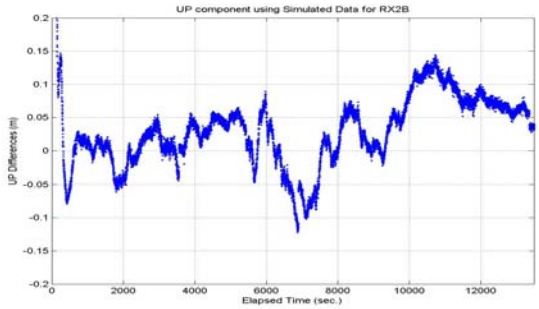

Figure 19. Simulated RX2B position solution once RX1B has been fixed.

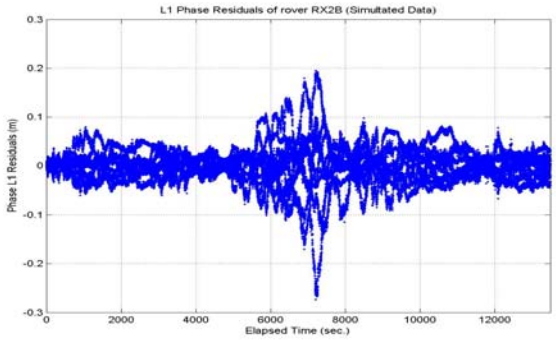

Figure 20. L1 double differenced residuals for the simulated RX2B and RX1B.

CONCLUSIONS AND FUTURE STUDY

In this paper, we demonstrated a new analysis method for common zenith-dependent parameters to decorrelate the vertical component and the tropospheric parameters. For this purpose, data from a severe localized tropospheric event were reprocessed to analyze our proposed method. As both the vertical component and the tropospheric parameters are all zenith dependent, we introduced a new common parameter to have them combined. For the purpose of investigating the possible positioning improvement under severe imbalanced atmospheric conditions, relevant parameters from Bernese were extracted and reprocessed using the designed software. In a short baseline with normal tropospheric conditions, the additional estimation of the tropospheric parameter may make the positioning solution unstable. This is because the introduction of another parameter in the estimation process may weaken the solution even though it is beneficial in reducing a certain type of bias or error. In order to avoid such difficulties, the new common parameter introduced combines the common zenith dependent parameters.

We investigated the possible positioning improvements after introducing the combined parameter in the processing of the data collected during severe inhomogeneous tropospheric conditions. In conclusion, the local troposphere anomaly is highly correlated with the height component. So, improper mitigation of that effect can severely degrade the vertical positioning performance even for short baselines (less than 10 km). As proposed, we introduced a new α and ζ coefficient for combining and decorrelating the cross dependent parameters. If the coefficient is properly selected, the combined zenith-dependent parameter greatly improves the positioning solution especially during a local tropospheric anomaly effect. The northing and easting component using the proposed method are also improved. The overall improvement in the positioning domain shows that the bias and standard deviation of height component are greatly reduced.

As the troposphere is a limiting factor for high precision positioning, an extensive analysis of the imbalanced anomaly cases is necessary. Unfortunately, it is almost impossible to record such data sets due to logistic problems. As a result, a series of imbalanced tropospheric phenomenon in a network is difficult to obtain from real networks. A simulation would be preferable in this case for extensive analysis of those impacts.

In this paper, we also demonstrated the simulation after performing quantitative analysis of all possible errors using real observables. With the errors estimated for each station involved, Spirent™ STR4760 L1/L2/L2C hardware simulators can be used for generating artificial observables to further analyze GPS positioning errors due to the severe tropospheric anomaly effects. We simulated those similar effects using the hardware simulator and generated similar error patterns. Based on many different tests using the simulated data, we can choose a realistic value of α for proper weighting to mitigate unwanted noise or errors.

ACKNOWLEDGMENTS

The authors would like to acknowledge the Natural Sciences and Engineering Research Council of Canada (NSERC), the Canada Foundation for Innovation (CFI) and the New Brunswick Innovation Foundation (NBIF) for support for the research. Some parts of the research reported in this paper were carried out under contract specifically for GNSS simulation system development for modeling environmental error. The support of the Korea Astronomy and Space Institute (KASI) is greatly acknowledged. The authors also thank the Astronomical Institute of University of Bern for the Bernese software, supported by the Royal Institution of Chartered Surveyors (RICS) Education Trust.

REFERENCES

Ahn, Y. W., D. Kim, P. Dare, and R. B. Langley (2005). "Long baseline GPS RTK performance in a marine environment using NWP ray-tracing technique under varying tropospheric conditions", Proceedings of ION GNSS 2005, Long Beach, California, U.S.A., pp 2092-2103.

Ahn, Y. W., D. Kim, and P. Dare (2006). "Local tropospheric anomaly effects on GPS RTK performance", *Proceedings of ION GNSS 2006*, Fort Worth, Texas, U.S.A, pp. 1925-1935

Ahn, Y.W., D. Kim, and P. Dare (2007). "Positioning Impacts from Imbalanced Atmospheric GPS Network Errors", *Proceedings of ION GNSS* 2007, Fort Worth, Texas, U.S.A, pp. 2302-2312.

Comparetto (1993). "The impact of dust and foliage on singal attenuation in the millimeter wave regime", *Journal of Space Communication,* Vol 11, no.1, pp.13-20.

Cove, K. (2005). "*Improvements in GPS tropospheric delay estimation with numerical weather prediction*" M.Sc.E Thesis, Department of Geodesy and Geomatics Engineering, University of New Brunswick, Canada.

Cove, K., M.C. Santos, D. Wells, S. Bisnah (2004). "Improved tropospheric delay estimation for long baseline, carrier phase differential GPS positioning in a coastal environment" *Proceeding of ION GNSS 2004*, Long Beach, CA, USA, pp 925-932.

Google (2008). Google maps, http://maps.google.ca [accessed in August, 2008].

Huang, J. and F. van Graas (2006). "Comparison of tropospheric decorrelation errors in the presence of severe weather conditions in different areas and over different baseline lengths", *Proceedings of ION GNSS 2006*, Fort Worth, Texas, U.S.A, pp. 2769-2787

Kim, D. and R. B. Langley (2007). "Long-Range Single-Baseline RTK for Complementing Network-based RTK", *Proceedings of ION GNSS 2007*, Fort Worth, Texas, U.S.A, pp. 639-650.

Lawrence D., R. B. Langley, D. Kim, F. Chan, and B. Pervan (2006). "Decorrelation of troposphere across short baseline", *IEEE/ION PLANS 2006*, San Diego, California, U.S.A, pp. 97-102

Leick, A. (1995). *GPS Satellite Surveying*, 2nd Ed. John Wiley & Sons, New York.

Mendes, V. B. and R. B. Langley (1995). "Zenith Wet Tropospheric Delay Determination Using Prediction Model: Accuracy Analysis", *Cartograpia e Cadastro*, Vol.2, pp. 41-47.

Nicholson, N. A., S. Skone, M. E. Cannon, G. Lachapelle, and N. Luo (2005). "Regional tropospheric tomography based on real-time double difference observables", *Proceedings of ION GNSS 2005*, Long Beach, California, U.S.A, pp 269-280.

Niell, A. E. (1996). "Global mapping functions for the atmosphere delay at radio wavelengths", *Journal of Geophysical Research*, Vol.101, No.B2, pp. 3227-3246.

Nievinski, F., K. Cove, M. Santos, D. Wells and R. Kingdon (2005). "Range-Extended GPS Kinematic Positioning using Numerical Weather Prediction Model" *Proceedings of ION Annual Meeting*, Boston, USA

Saastamoinen, J. (1972). "Atmospheric correction for troposphere and stratosphere in radio ranging satellites", Geophysical monograph, 15, *American Geophysical Union*, Washington, D. C., USA, pp. 247-252.

Skone, S. and S. Shrestha (2003). "4-D modeling of water vapor using a regional GPS network", *Proceedings of the ION National Technical Meeting*, Anaheim, California, U.S.A.

Unisys (2005). Unisys weather, http://weather.unisys.com/.

Zhang, Y. and C. Bartone (2006). "Single-site carrier phase based troposphere integrity monitoring", *Proceedings of ION National Technical Meeting*, San Diego, California, U.S.A, pp. 530-542.